Research Paper
Computational Methods for Differential Equations
http://cmde.tabrizu.ac.ir
Vol. *, No. *, *, pp. 1-20
DOI:10.22034/cmde.2025.66734.3149

Computational analysis of fractal-fractional differential systems via Vieta-Lucas fractal-fractional operational matrices

Rakesh Kumar[1], **Shivani Aeri**[1,*], **and Dumitru Baleanu**[2,3]

[1]School of Mathematics, Computers and Information Sciences, Central University of Himachal Pradesh, Shahpur Campus, Shahpur 176206, India.

[2]Department of Computer Science and Mathematics, Lebanese American University, Beirut, Lebanon.

[3]Institute of Space Sciences, Magurele-Bucharest, Romania.

Abstract

Fractal-fractional differential equations are important as they can help to model the real-world systems that have memory effects and thus find their existence in various real-world phenomena such as physics, engineering, biology, and biomedicine. It is always challenging to handle the fractal-fractional derivatives using traditional numerical methods, which motivates the need to develop the numerical methods that can handle these fractal-fractional models accurately and effectively. In this work, a novel numerical scheme, the Vieta-Lucas fractal fractional matrix ($VLFF$) method, is presented for solving the system of fractal-fractional differential equations (FFDEs). The operational matrices for derivative and fractal fractional derivatives of Vieta-Lucas polynomials over the generalized domain are constructed. Making use of the fractal-fractional operational matrix technique streamlines the computation processes and significantly reduces the challenges while dealing with fractal-fractional derivatives. This simplified matrix method is then applied with the Tau approach to find the solution of a system of FFDEs. Further, the geometric representation of the fractal-fractional derivative matrix is presented, showcasing the fractal patterns. The proposed method is validated through numerous examples, with solution curves and error analysis presented for different fractal and fractional orders. A comparison has been made with the existing numerical methods to validate the accuracy and reliability of the proposed $VLFF$ method.

Keywords. Fractal-fractional differential equations, Vieta-Lucas polynomials, Operation matrix, Tau method, Numerical solution.
2010 Mathematics Subject Classification. 65L10, 33C47, 41A10.

1. Introduction

The development of fractional calculus marks a crucial advancement in scientific communities as its mathematical models incorporate memory and hereditary properties of complex structured systems. Fractal-fractional derivatives serve to unify fractional calculus and fractal geometry research approaches as they facilitate the analysis of fractal structures with nonlocal features [5]. This methodology demonstrates broad utility in viscoelasticity, fluid dynamics, and anomalous diffusion research. Fractal-fractional calculus is a complex mathematical tool that clarifies the physical phenomena associated with fractal dynamics and fractional geometry. Fractal-fractional differential equations (FFDEs) integrate fractal and fractional concepts to develop effective modeling instruments for examining systems that necessitate memory effects, multi-scale processes, and self-similar structures [11]. Fractal-fractional derivatives uniquely integrate memory effects, heterogeneity, and fractal geometry, rendering them indispensable for the analysis of dynamic systems, in contrast to integer-order derivatives, which fail to encapsulate such complex dynamics. FFDEs represent a significant advancement in mathematical modeling as they establish enhanced analytical frameworks for the investigation of complex processes exhibiting irregular and fractal behavior [1]. Biological processes necessitate the utilization of FFDEs as modeling tools for their analysis and interpretation in biological systems. A detailed convergence framework for tumor immune models using distinct kernels is provided in [19], while efficient computational

Received: 12 April 2025; Accepted: 14 April 2026.
∗ Corresponding author. Email: shivvani.aeri@gmail.com.

techniques for solving fractal differential systems are developed in [17]. FFDEs enable epidemiological researchers to simulate disease transmission patterns for COVID-19 [16] and HIV/HCV [15]. Incorporating fractal-fractional operators, these models yield enhanced insights into infection dynamics and assist in formulating effective preventative methods. FFDEs are employed in fluid dynamics to characterize non-linear viscoelastic fluids, especially in scenarios where traditional models fall short, such as in porous medium [14].

Analytical solutions or approximate solutions for FFDEs are frequently challenging due to their complexity, the fractal-fractional order derivatives involved, and the need to create dependable numerical methods. Numerous researchers work on the numerical methods for the solutions of FFDEs such as inverse Laplace transform [3], and Laplace variational iteration method [10]. The operational matrix method is an efficient numerical technique for solving fractional and fractal-fractional differential equations [6, 20]. The essential operational matrix methods for solving a diverse range of FFDEs are the Bernstein matrix method [23], Haar wavelet matrix method [12], Vieta-Fibonacci method [21], Legendre polynomial method [18] and Fractional PINN's with operational matrices [24]. Although operational matrix approaches provide considerable computing benefits, they need a meticulous selection of basis functions and operational matrices to guarantee precision and efficacy.

This paper seeks to examine the dynamic behavior of a system of differential equations modeled using the Caputo fractal-fractional derivative by developing a numerical framework utilizing the Vieta-Lucas fractal-fractional matrix approach. To the best of the author's knowledge, this kind of numerical framework utilizing Vieta-Lucas polynomials over the generalized domain for solving the system of FFDEs has not been developed yet. The operational matrices of fractal-fractional derivatives have been developed for the shifted Vieta-Lucas polynomials and the Tau method is further incorporated to solve the algebraic equations obtained. The structure of the paper is as follows: Section 2 provides the basic preliminaries such as fractal-fractional definitions, Vieta-Lucas polynomials, and its shifted version. In section 3, the operational matrices of ordinary derivative and fractal-fractional derivatives are derived over the generalized domain and their geometrical representations are presented. The mathematical implementation of the proposed $VLFF$ method to solve the system of FFDEs is presented in section 4. Numerous test examples are tested and a comparative study has been done to validate the method's accuracy and reliability in section 5. Further, the concluding remarks are presented in section 6.

2. Preliminaries

To help with the investigation of fractal-fractional models, we examine the fundamentals of fractal-fractional calculus in this part. The basic definitions in fractal-fractional calculus are presented, along with Vieta-Lucas polynomials and their shifted version, emphasizing some of their interesting characteristics.

Definition 2.1. Let $\Gamma(\xi)$ represents the gamma function defined as follows [22]:

$$\Gamma(\xi) = \int_0^\infty e^{-\tau}\tau^{\xi-1}d\tau,\ \xi \in \mathbb{C},\ \mathbb{R}(\xi) > 0. \tag{2.1}$$

Definition 2.2. Let $B(\xi_1, \xi_2)$ represents the beta function given as [22]:

$$B(\xi_1, \xi_2) = \int_0^1 \tau^{\xi_1-1}(1-\tau)^{\xi_2-1}d\tau,\ \xi_1, \xi_2 \in \mathbb{C},\ \mathbb{R}(\xi_1), \mathbb{R}(\xi_2) > 0. \tag{2.2}$$

Definition 2.3. Consider $\psi(\xi)$ be fractal differentiable of order $\beta \in (0, 1]$ such that $\psi : [0, l] \to \mathbb{R}$. The Caputo fractal fractional differentiation of order (α, β) is defined as [4]:

$${}_0^{Cff}D_\xi^{\alpha,\beta}\psi(\xi) = \frac{1}{\Gamma(1-\alpha)}\int_0^\xi \frac{d\psi(\eta)}{d\eta^\beta}(\xi-\eta)^{-\alpha}d\eta,\ \alpha, \beta \in (0, 1]. \tag{2.3}$$

In this case, the fractal order is β, while the fractional order is α. In addition, we have

$$\frac{d\psi(\eta)}{d\eta^\beta} = \lim_{\xi\to\eta}\frac{\psi(\xi)-\psi(\eta)}{\xi^\beta-\eta^\beta} = \beta^{-1}\eta^{1-\beta}\frac{d}{d\eta}\psi(\eta). \tag{2.4}$$

Lemma 2.1. *Let $r \in \mathbb{N} \cup \{0\}$, $\mu \in \mathbb{R}$ and $\alpha, \beta \in (0,1]$, then the Caputo fractal fractional differentiation of some elementary functions are given as follows [7]:*

$$
\begin{aligned}
{}_0^{Cff}D_\xi^{\alpha,\beta}\xi^r &= \begin{cases} 0, & r=0 \\ \frac{r\Gamma(r+1-\beta)}{\beta\Gamma(r+2-\alpha-\beta)}\xi^{r+1-\alpha-\beta}, & r \in \mathbb{N}. \end{cases} \\
{}_0^{Cff}D_\xi^{\alpha,\beta}e^{\mu\xi} &= \frac{\mu\ \xi^{2-\alpha-\beta}}{\beta}\sum_{p=0}^{\infty}\frac{\Gamma(p-\beta+2)}{p!\ \Gamma(p-\alpha-\beta+3)}(\mu\xi)^p, \\
{}_0^{Cff}D_\xi^{\alpha,\beta}e^{-\mu\xi} &= -\frac{\mu\ \xi^{2-\alpha-\beta}}{\beta}\sum_{p=0}^{\infty}\frac{\Gamma(p-\beta+2)}{p!\ \Gamma(p-\alpha-\beta+3)}(-\mu\xi)^p, \\
{}_0^{Cff}D_\xi^{\alpha,\beta}\sin(\mu\xi) &= \frac{\mu\ \xi^{2-\alpha-\beta}}{\beta}\sum_{p=0}^{\infty}\frac{\Gamma(2p-\beta+2)}{(2p)!\ \Gamma(2p-\alpha-\beta+3)}(-\mu\xi^2)^p, \\
{}_0^{Cff}D_\xi^{\alpha,\beta}\cos(\mu\xi) &= \frac{-\mu^2\ \xi^{3-\alpha-\beta}}{\beta}\sum_{p=0}^{\infty}\frac{\Gamma(2p-\beta+3)}{(2p+1)!\ \Gamma(2p-\alpha-\beta+4)}(-\mu\xi^2)^p.
\end{aligned}
\tag{2.5}
$$

Definition 2.4. The Vieta-Lucas polynomials over $[-2,2]$ of degree s can be defined as [9]:

$$vl_s(\xi) = 2\cos(s\delta), \tag{2.6}$$

where $s \in \mathbb{N} \cup \{0\}$, $\delta = \arccos\left(\frac{\xi}{2}\right)$ and $\delta \in [0,\pi]$.

A variable transformation is used to produce the shifted Vieta-Lucas (SVL) polynomials, which are defined across the interval $[0,l]$. These SVL polynomials are represented as $vl_s\left(\frac{4}{l}\xi-2\right)$ and are identified as $\mathcal{VL}_{l,s}(\xi)$. Their derivation stems from the following relationship [2]:

$$\mathcal{VL}_{l,s}(\xi) = \left(\frac{4}{l}\xi-2\right)\mathcal{VL}_{l,s-1}(\xi) - \mathcal{VL}_{l,s-2}(\xi),\ s \geq 2. \tag{2.7}$$

with $\mathcal{VL}_{l,0}(\xi) = 2$ and $\mathcal{VL}_{l,1}(\xi) = 4\xi - 2$.
For SVL polynomials, the power series expression is as follows [8]:

$$\mathcal{VL}_{l,s}(\xi) = 2s\sum_{j=0}^{s}(-1)^{s-j}\frac{4^j\Gamma(s+j)}{\Gamma(2j+1)\Gamma(s-j+1)}\left(\frac{\xi}{l}\right)^j, \quad s \geq 1. \tag{2.8}$$

The orthogonality condition with weight function $\omega_l(\xi) = \frac{1}{\sqrt{l\xi-\xi^2}}$ is given as [2]:

$$\langle \mathcal{VL}_{l,s}(\xi), \mathcal{VL}_{l,m}(\xi)\rangle_{\omega_l(\xi)} = \int_0^1 \mathcal{VL}_{l,s}(\xi)\mathcal{VL}_{l,m}(\xi)\omega_l(\xi)\,d\xi = \begin{cases} 4\pi, & s=m=0, \\ 2\pi, & s=m\neq 0, \\ 0, & s\neq m\neq 0. \end{cases} \tag{2.9}$$

Functional approximation:

Consider $\psi(\xi) \in L^2_\omega([0,l])$ can be expanded in terms of SVL polynomials as [13]:

$$\psi(\xi) = \sum_{s=0}^{\infty} z_s \mathcal{VL}_{l,s}(\xi), \tag{2.10}$$

where

$$z_s = \frac{1}{\gamma_s\pi}\int_0^l \omega_l(\xi)\psi(\xi)\mathcal{VL}_{l,s}(\xi)d\xi, \quad s \geq 0, \tag{2.11}$$

for

$$\gamma_s = \begin{cases} 4, & s = 0, \\ 2, & s \geq 1. \end{cases}$$

The truncated expansion is given as:

$$\psi(\xi) \simeq \sum_{s=0}^{m} c_s \mathcal{VL}_{l,s}(\xi) \triangleq C^T \phi_{l,m+1}(\xi), \tag{2.12}$$

where

$$Z = [z_0, z_1, z_2, \ldots, z_m]^T, \qquad \phi_{l,m+1}(\xi) = [\mathcal{VL}_{l,0}(\xi), \mathcal{VL}_{l,1}(\xi), \mathcal{VL}_{l,2}(\xi), \ldots, \mathcal{VL}_{l,m}(\xi)]^T. \tag{2.13}$$

3. Fractal-fractional matrix and geometrical variations

Theorem 3.1. *(Ordinary derivative matrix) Let $\phi_{l,m+1}(\xi)$ be a SVL polynomials vector defined in Eq. (2.13), then we have*

$$\frac{d\phi_{l,m+1}(\xi)}{d\xi} \simeq D^{(1)}_{l,m+1} \phi_{l,m+1}(\xi),$$

where $D^{(1)}_{l,m+1}$ represents the derivative operational matrix and is expressed as follows:

$$D^{(1)}_{l,m+1} = \begin{pmatrix} 0 & 0 & \cdots & 0 \\ \Upsilon_{1,0} & \Upsilon_{1,1} & \cdots & \Upsilon_{1,m} \\ \vdots & \vdots & \ddots & \vdots \\ \Upsilon_{m,0} & \Upsilon_{m,1} & \cdots & \Upsilon_{m,m} \end{pmatrix},$$

where $\Upsilon_{p,s}$ is given by:

$$\Upsilon_{p,s} = \begin{cases} \sum_{i=1}^{p} (-1)^{p-i} \frac{4^i i p \Gamma(p+i)\Gamma(i-\frac{1}{2})}{\sqrt{\pi} l \Gamma(2i+1)\Gamma(p-i+1)\Gamma(i)}, & s = 0, \\ \sum_{i=1}^{p} \sum_{j=0}^{s} 2(-1)^{p+s-i-j} \frac{4^{i+j} s p i \Gamma(p+i)\Gamma(s+j)\Gamma(i+j-\frac{1}{2})}{\sqrt{\pi} l \Gamma(2i+1)\Gamma(p-i+1)\Gamma(2j+1)\Gamma(s-j+1)\Gamma(i+j)}, & s \geq 1. \end{cases}$$

Proof. For $p = 0$, we have $\frac{d\mathcal{VL}_{l,0}(\xi)}{d\xi} = 0$. So the elements in the first row of the matrix $D^{(1)}_{l,m+1}$ should be zero. For $p \geq 1$, we have

$$\begin{aligned} \frac{d\mathcal{VL}_{l,p}(\xi)}{d\xi} &= 2p \sum_{i=0}^{p} (-1)^{p-i} \frac{4^i \Gamma(p+i)}{\Gamma(2i+1)\Gamma(p-i+1)} \frac{d}{d\xi} \left(\frac{\xi}{l}\right)^i \\ &= 2p \sum_{i=1}^{p} (-1)^{p-i} \frac{4^i i \Gamma(p+i)}{l^i \Gamma(2i+1)\Gamma(p-i+1)} \xi^{i-1}. \end{aligned} \tag{3.1}$$

The SVL polynomials can express the above equations' power functions as:

$$\xi^{i-1} = \sum_{s=0}^{m} c_{is} \mathcal{VL}_{l,s}(\xi), \tag{3.2}$$

where

$$c_{is} = \frac{1}{\gamma_s \pi} \int_0^l \omega_l(\xi) \xi^{i-1} \mathcal{VL}_{l,s}(\xi) d\xi \tag{3.3}$$

$$\gamma_s = \begin{cases} 4, & s = 0, \\ 2, & s \geq 1. \end{cases}$$

Substituting the values of γ_s and $\mathcal{VL}_{l,s}(\xi)$, we get

$$c_{is} = \begin{cases} \frac{1}{4\pi}\int_0^l \frac{2\xi^{i-1}}{\sqrt{l\xi-\xi^2}}d\xi, & s=0, \\ \frac{1}{2\pi}\int_0^l \frac{\xi^{i-1}}{\sqrt{l\xi-\xi^2}}2s\sum_{j=0}^{s}(-1)^{s-j}\frac{4^j\Gamma(s+j)}{\Gamma(2j+1)\Gamma(s-j+1)}\left(\frac{\xi}{l}\right)^j d\xi, & s\geq 1. \end{cases}$$

$$c_{is} = \begin{cases} \frac{1}{2\pi}\int_0^l \frac{\xi^{i-1}}{\sqrt{l\xi-\xi^2}}d\xi, & s=0, \\ \frac{1}{\pi}\int_0^l \sum_{j=0}^{s}(-1)^{s-j}\frac{s4^j\Gamma(s+j)}{l^j\Gamma(2j+1)\Gamma(s-j+1)}\frac{\xi^{i+j-1}}{\sqrt{l\xi-\xi^2}}d\xi, & s\geq 1. \end{cases}$$

$$c_{is} = \begin{cases} \frac{1}{2\sqrt{\pi}}\frac{l^{i-1}\Gamma(i-\frac{1}{2})}{\Gamma(i)}, & s=0, \\ \frac{1}{\sqrt{\pi}}\sum_{j=0}^{s}(-1)^{s-j}\frac{s4^j\Gamma(s+j)}{\Gamma(2j+1)\Gamma(s-j+1)}\frac{l^{i-1}\Gamma(i+j-\frac{1}{2})}{\Gamma(i+j)}, & s\geq 1. \end{cases}$$

Using the values of ξ^{i-1}, we have

$$\frac{d\mathcal{VL}_{l,s}(\xi)}{d\xi} = \sum_{s=0}^{m}\Upsilon_{p,s}\mathcal{VL}_{l,s}(\xi), \tag{3.4}$$

where

$$\Upsilon_{p,s} = \begin{cases} \sum_{i=1}^{p}(-1)^{p-i}\frac{4^i ip\Gamma(p+i)\Gamma(i-\frac{1}{2})}{\sqrt{\pi}l\Gamma(2i+1)\Gamma(p-i+1)\Gamma(i)}, & s=0, \\ \sum_{i=1}^{p}\sum_{j=0}^{s}2(-1)^{p+s-i-j}\frac{4^{i+j}ips\Gamma(p+i)\Gamma(s+j)\Gamma(i+j-\frac{1}{2})}{\sqrt{\pi}l\Gamma(2i+1)\Gamma(p-i+1)\Gamma(2j+1)\Gamma(s-j+1)\Gamma(i+j)}, & s\geq 1, \end{cases}$$

which completes the proof.

□

Lemma 3.2. *The n^{th} order derivative of the vector $\phi_{l,m+1}(\xi)$ is given as follows [6]:*

$$\frac{d^n\phi_{l,m+1}(\xi)}{d\xi^n} = \underbrace{D^{(1)}_{l,m+1}\times D^{(1)}_{l,m+1}\times\cdots\times D^{(1)}_{l,m+1}}_{n\ times}\phi_{l,m+1}(\xi) \triangleq D^{(n)}_{l,m+1}\phi_{l,m+1}(\xi). \tag{3.5}$$

As a numerical example, we have

$$D^{(1)}_{4,6} = \frac{1}{2}\begin{pmatrix} 0 & 0 & 0 & 0 & 0 & 0 \\ 1 & 0 & 0 & 0 & 0 & 0 \\ 0 & 4 & 0 & 0 & 0 & 0 \\ 3 & 0 & 6 & 0 & 0 & 0 \\ 0 & 8 & 0 & 8 & 0 & 0 \\ 5 & 0 & 10 & 0 & 10 & 0 \end{pmatrix}, D^{(2)}_{4,6} = \frac{1}{4}\begin{pmatrix} 0 & 0 & 0 & 0 & 0 & 0 \\ 0 & 0 & 0 & 0 & 0 & 0 \\ 4 & 0 & 0 & 0 & 0 & 0 \\ 0 & 24 & 0 & 0 & 0 & 0 \\ 32 & 0 & 48 & 0 & 0 & 0 \\ 0 & 120 & 0 & 80 & 0 & 0 \end{pmatrix}.$$

Theorem 3.3. *(Fractal-fractional derivative matrix) Let $\phi_{l,m+1}(\xi)$ be a SVL polynomials vector defined in Eq. (2.13) and $\alpha,\beta\in(0,1]$, then we have*

$${}^{Cff}_{0}D^{\alpha,\beta}_{\xi}\phi_{l,m+1}(\xi) \simeq G^{(\alpha,\beta)}_{l,m+1}\phi_{l,m+1}(\xi),$$

where $G^{(\alpha,\beta)}_{l,m+1}$ *represents the fractal-fractional derivative operational matrix and is expressed as follows:*

$$G^{(\alpha,\beta)}_{l,m+1} = \begin{pmatrix} 0 & 0 & \cdots & 0 \\ \upsilon_{1,0} & \upsilon_{1,1} & \cdots & \upsilon_{1,m} \\ \vdots & \vdots & \ddots & \vdots \\ \upsilon_{m,0} & \upsilon_{m,1} & \cdots & \upsilon_{m,m} \end{pmatrix},$$

where $\upsilon_{p,s}$ *is given by:*

$$\upsilon_{p,s} = \begin{cases} \sum_{i=1}^{p}(-1)^{p-i}\frac{4^i ip\Gamma(p+i)\Gamma(i-\beta+1)\Gamma(\frac{3}{2}-\alpha-\beta+i)}{\sqrt{\pi}l^{\alpha+\beta-1}\beta\Gamma(2i+1)\Gamma(p-i+1)\Gamma(i-\alpha-\beta+2)\Gamma(2-\alpha-\beta+i)}, & s=0, \\ \sum_{i=1}^{p}\sum_{j=0}^{s}2(-1)^{p+s-i-j}\frac{4^{i+j}ips\Gamma(p+i)\Gamma(s+j)\Gamma(i-\beta+1)\Gamma(\frac{3}{2}-\alpha-\beta+i+j)}{\sqrt{\pi}l^{\alpha+\beta-1}\beta\Gamma(2i+1)\Gamma(p-i+1)\Gamma(2j+1)\Gamma(s-j+1)\Gamma(i-\alpha-\beta+2)\Gamma(2-\alpha-\beta+i+j)}, & s\geq 1, \end{cases}$$

Proof. Using Eqs. (2.5) and (2.7), we have ${}^{Cff}_{0}D^{\alpha,\beta}_{\xi}\mathcal{VL}_{l,0}(\xi) = 0$. So the elements in the first row of the matrix $D^{(\alpha,\beta)}_{l,m+1}$ should be zero. For $p \geq 1$, we have

$$\begin{aligned} {}^{Cff}_{0}D^{\alpha,\beta}_{\xi}\mathcal{VL}_{l,p}(\xi) &= 2p\sum_{i=0}^{p}(-1)^{p-i}\frac{4^i\Gamma(p+i)}{\Gamma(2i+1)\Gamma(p-i+1)}\,{}^{Cff}_{0}D^{\alpha,\beta}_{\xi}\left(\frac{\xi}{l}\right)^i \\ &= 2p\sum_{i=1}^{p}(-1)^{p-i}\frac{4^i i\Gamma(p+i)}{l^i\beta\Gamma(2i+1)\Gamma(p-i+1)}\frac{\Gamma(i-\beta+1)}{\Gamma(i-\alpha-\beta+2)}\xi^{i-\alpha-\beta+1}. \end{aligned} \tag{3.6}$$

The SVL polynomials can express the power functions in the above equations as:

$$\xi^{i-\alpha-\beta+1} = \sum_{s=0}^{m} c_{is}\mathcal{VL}_{l,s}(\xi), \tag{3.7}$$

where

$$c_{is} = \frac{1}{\gamma_s\pi}\int_0^l \omega_l(\xi)\xi^{i-\alpha-\beta+1}\mathcal{VL}_{l,s}(\xi)d\xi \tag{3.8}$$

$$\gamma_s = \begin{cases} 4, & s=0, \\ 2, & s\geq 1. \end{cases}$$

Substituting the values of γ_s and $\mathcal{VL}_{l,s}(\xi)$, we get

$$c_{is} = \begin{cases} \frac{1}{4\pi}\int_0^l \frac{2\xi^{i-\alpha-\beta+1}}{\sqrt{l\xi-\xi^2}}d\xi, & s=0, \\ \frac{1}{2\pi}\int_0^l \frac{\xi^{i-\alpha-\beta+1}}{\sqrt{l\xi-\xi^2}}2s\sum_{j=0}^{s}(-1)^{s-j}\frac{4^j\Gamma(s+j)}{\Gamma(2j+1)\Gamma(s-j+1)}\left(\frac{\xi}{l}\right)^j d\xi, & s\geq 1. \end{cases}$$

$$c_{is} = \begin{cases} \frac{1}{2\pi}\int_0^l \frac{\xi^{i-\alpha-\beta+1}}{\sqrt{l\xi-\xi^2}}d\xi, & s=0, \\ \frac{1}{\pi}\int_0^l \sum_{j=0}^{s}(-1)^{s-j}\frac{s4^j\Gamma(s+j)}{l^j\Gamma(2j+1)\Gamma(s-j+1)}\frac{\xi^{i+j-\alpha-\beta+1}}{\sqrt{l\xi-\xi^2}}d\xi, & s\geq 1. \end{cases}$$

$$c_{is} = \begin{cases} \frac{1}{2\sqrt{\pi}}\frac{l^{i-\alpha-\beta+1}\Gamma(\frac{3}{2}-\alpha-\beta+i)}{\Gamma(2-\alpha-\beta+i)}, & s=0, \\ \frac{1}{\sqrt{\pi}}\sum_{j=0}^{s}(-1)^{s-j}\frac{s4^j\Gamma(s+j)}{\Gamma(2j+1)\Gamma(s-j+1)}\frac{l^{i-\alpha-\beta+1}\Gamma(\frac{3}{2}-\alpha-\beta+i+j)}{\Gamma(2-\alpha-\beta+i+j)}, & s\geq 1. \end{cases}$$

Using the values of $\xi^{i-\alpha-\beta+1}$, we have

$$\frac{d\mathcal{VL}_{l,s}(\xi)}{d\xi} = \sum_{s=0}^{m} \upsilon_{p,s}\mathcal{VL}_{l,s}(\xi) \tag{3.9}$$

where

$$\upsilon_{p,s} = \begin{cases} \sum_{i=1}^{p}(-1)^{p-i}\frac{4^i ip\Gamma(p+i)\Gamma(i-\beta+1)\Gamma(\frac{3}{2}-\alpha-\beta+i)}{\sqrt{\pi}l^{\alpha+\beta-1}\beta\Gamma(2i+1)\Gamma(p-i+1)\Gamma(i-\alpha-\beta+2)\Gamma(2-\alpha-\beta+i)}, & s=0, \\ \sum_{i=1}^{p}\sum_{j=0}^{s}\frac{2(-1)^{p+s-i-j}4^{i+j}ips\Gamma(p+i)\Gamma(s+j)\Gamma(i-\beta+1)\Gamma(\frac{3}{2}-\alpha-\beta+i+j)}{\sqrt{\pi}l^{\alpha+\beta-1}\beta\Gamma(2i+1)\Gamma(p-i+1)\Gamma(2j+1)\Gamma(s-j+1)\Gamma(i-\alpha-\beta+2)\Gamma(2-\alpha-\beta+i+j)}, & s\geq 1, \end{cases}$$

which completes the proof. □

As a numerical illustration, we obtain

$$G_{4,6}^{(\frac{1}{4},\frac{1}{2})} = \begin{pmatrix} 0 & 0 & 0 & 0 & 0 & 0 \\ 2.02501 & 2.25001 & 0.17307 & -0.03054 & 0.01018 & -0.00447 \\ 0.30000 & 2.63079 & 2.72852 & 0.28507 & -0.06027 & 0.02263 \\ 0.62973 & 0.63733 & 2.53508 & 3.04821 & 0.35720 & -0.08210 \\ 0.29466 & 1.07345 & 0.66244 & 2.56029 & 3.29277 & 0.40991 \\ 0.42824 & 0.57104 & 1.01399 & 0.68564 & 2.61342 & 3.49326 \end{pmatrix}.$$

Geometric representation of fractal-fractional derivative matrix:

In this part, the geometric representation of the fractal-fractional derivative matrix is analyzed for different values of fractional order α and fractal order β to highlight their geometrical significance. The 3D visualization of the fractal-fractional derivative matrix is given in Figure 1 and the zoom profile of the contour plots is provided in Figure 2, showcasing the fractal patterns formation.

The three-dimensional (3D) visualization of the fractal-fractional matrix is presented in Figures 1(a), 1(b), and 1(c) for a fixed fractional order α and varying fractal order β. These plots help to showcase the behavior of the operational matrix when the fractal order is varied. Similarly, for a fixed fractal order β and varying fractional order α, the 3D visualization of the fractal-fractional matrix is presented in Figures 1(d), 1(e) and 1(f), highlighting the characteristics of fractional order component. Furthermore, Figures 1(g), 1(h), and 1(i) present the operational matrix plots for varying fractal and fractional order specifically where $\alpha = \beta$.

The zoom profile of the contour plots for the fractal-fractional operational matrix is presented in Figure 2 for providing further insights into the fractal patterns form. For fixed fractional order α and varying fractal order β, the contour plots of the fractal-fractional matrix are presented in Figures 2(a), and 2(b). Similarly, for a fixed fractal order β and varying fractional order α, the contour plots of the fractal-fractional matrix are presented in Figures 2(c), and 2(d). Moreover, contour plots for varying fractal and fractional order for $\alpha = \beta$ are presented in Figures 2(e), and 2(f).

4. Mathematical model and implementation of numerical scheme

This section provides the mathematical framework for solving the system of fractal-fractional differential equations via the Vieta-Lucas fractal-fractional matrix method. For simplicity, let us consider the linear system of fractal-fractional differential equations as:

$$\begin{aligned} {}_0^{Cff}D_\xi^{\alpha_1,\beta_1}\psi_1(\xi) + \sum_{i=1}^{p} a_{1i}\psi_i(\xi) &= f_1(\xi), \\ {}_0^{Cff}D_\xi^{\alpha_2,\beta_2}\psi_2(\xi) + \sum_{i=1}^{p} a_{2i}\psi_i(\xi) &= f_2(\xi), \\ &\vdots \end{aligned} \tag{4.1}$$

.

$$ {}_{0}^{Cff}D_{\xi}^{\alpha_p,\beta_p}\psi_p(\xi)+\sum_{i=1}^{p} a_{pi}\psi_i(\xi) = f_p(\xi), $$

under the initial conditions

$$ \psi_i(0) = h_i,\ i = 1, 2, \cdots p, \tag{4.2} $$

where ${}_{0}^{Cff}D_{\xi}^{\alpha,\beta}$ represents the Caputo fractal-fractional derivative with α be the fractional order and β be the fractal order. The terms a_{1i}, a_{2i}, $\cdots$, a_{pi}, and h_i represents the real valued constants.

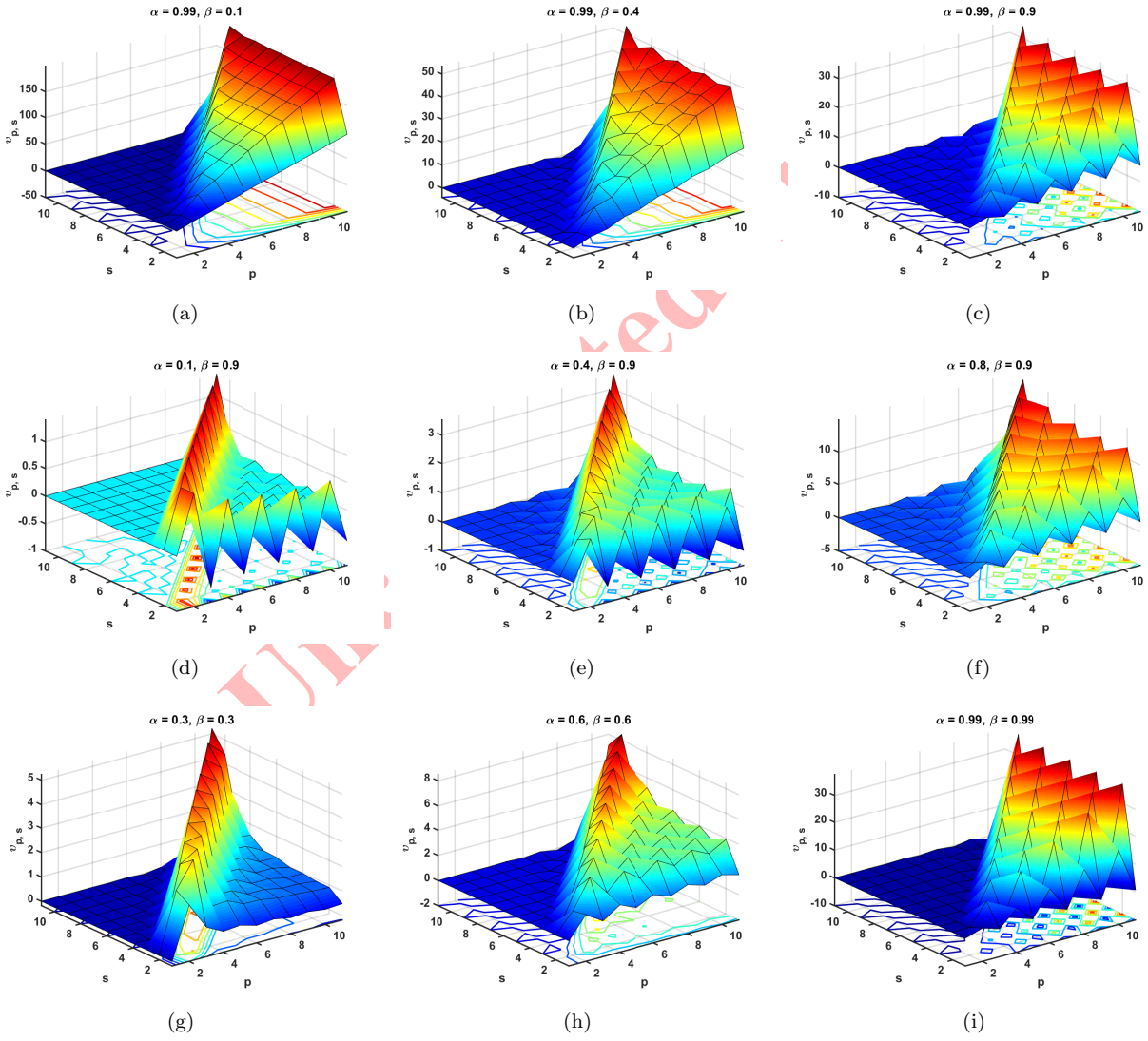

FIGURE 1. Geometric representation of fractal-fractional derivative matrix via 3D plots.

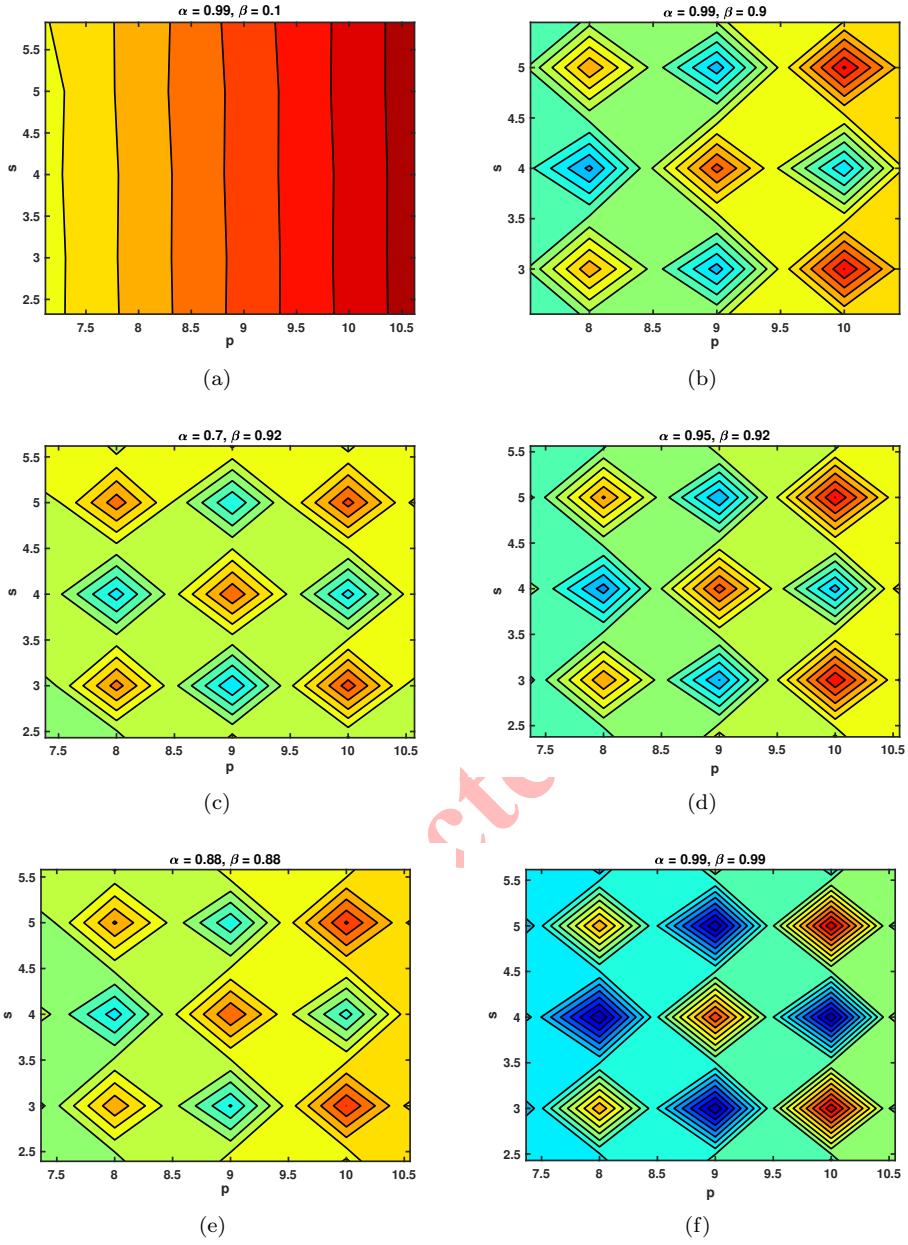

FIGURE 2. Contour plots for fractal-fractional derivative matrix.

The approximate solution $\psi_i(\xi)$ and the right-hand side $f_i(\xi)$ are represented using SVL polynomials as follows:

$$\psi_i(\xi) \simeq \sum_{s=0}^{m} z_{is} \mathcal{VL}_s(\xi) = Z_i^T \phi_{l,m+1}(\xi), \tag{4.3}$$

$$f_i(\xi) \simeq \sum_{s=0}^{m} f_{is} \mathcal{VL}_s(\xi) = F_i^T \phi_{l,m+1}(\xi), \tag{4.4}$$

where $Z_i = [z_{i0}, z_{i1}, \ldots, z_{im}]^T$ is unknown vector, $F_i = [f_{i0}, f_{i1}, \ldots, f_{im}]^T$ is known vector and $\phi_{l,m+1}(\xi) = [\mathcal{VL}_0(\xi), \mathcal{VL}_1(\xi), \ldots, \mathcal{VL}_m(\xi)]^T$.

The fractal-fractional derivative approximation for fractional order α_i and fractal order β_i is given as follows:

$$ {}_0^{Cff}D_\xi^{\alpha_i,\beta_i}\psi_i(\xi) \simeq Z_i^T G_{l,m+1}^{(\alpha_i,\beta_i)}\phi_{l,m+1}(\xi),\ i = 1, 2, \cdots, p. \tag{4.5} $$

Substituting Equations (4.3), (4.4), and (4.5) in system of FFDEs given in Equation (4.1) leads to residual equations as:

$$ R_i(\xi) = (Z_i^T G_{l,m+1}^{(\alpha_i,\beta_i)}\phi_{l,m+1}(\xi) + \sum_{j=1}^{p} a_{ij} Z_i^T - F_i^T)\phi_{l,m+1}(\xi), \qquad i = 1, 2, \cdots, p. \tag{4.6} $$

Boundary conditions are incorporated as:

$$ \psi_i(0) = Z_i^T \phi_{l,m+1}(0) = h_i,\ i = 1, 2, \cdots p. \tag{4.7} $$

Further, the Tau method transforms this residual system into a set of algebraic equations. Solving these equations provides the coefficients Z_i, from which the solutions $\psi_i(\xi)$ are obtained.

Algorithm 1

Input: a_{ij}, p and f_i.
Step I: Assume the approximate solution $\psi_i(\xi)$ in the form of $Z_i^T\phi_{l,m+1}(\xi)$.
Step II: Compute the operational matrix $G_{l,m+1}^{(\alpha_i,\beta_i)}$.
Step III: Substitute approximations into the residual system.
Step IV: Apply the Tau method to form algebraic equations.
Step V: Solve the equations numerically to determine Z_i.
Step VI: Construct the approximate solution $\psi_i(\xi) = Z_i^T\phi_{l,m+1}(\xi)$.
Output: The approximate solutions $\psi_i(\xi)$ for $i = 1, 2, \ldots, p$.

5. Numerical illustrations

Example 5.1. Let us take the system of FFDEs as follows:

$$ \begin{aligned} {}_0^{Cff}D_\xi^{\alpha_1,\beta_1}\psi_1(\xi) &= \psi_1(\xi) + \psi_2(\xi), \\ {}_0^{Cff}D_\xi^{\alpha_2,\beta_2}\psi_2(\xi) &= -\psi_1(\xi) + \psi_2(\xi), \end{aligned} \tag{5.1} $$

subject to

$$ \psi_1(0) = 0, \psi_2(0) = 1. \tag{5.2} $$

The exact solution was given as $\psi_1(\xi) = e^\xi \sin(\xi)$ and $\psi_2(\xi) = e^\xi \cos(\xi)$. The proposed $VLFF$ method has been used to solve the system of FFDEs stated in Example 5.1. To provide a better understanding of the influence of fractional and fractal components, the solution curves for $\psi_1(\xi)$ and $\psi_2(\xi)$ are presented in Figure 3 at different values of $\alpha_1, \alpha_2, \beta_1 \& \beta_2$. For fixed fractional orders $\alpha_1 = \alpha_2 = 0.99$ and varying fractal orders $\beta_1 = \beta_2 = 0.99, 0.95, 0.90, 0.85$, the solutions are presented in Figures 3(a) and 3(b). These plots help to showcase the impact of fractal order on the behavior of the solutions $\psi_1(\xi)$ and $\psi_2(\xi)$. Similarly, for fixed fractal orders $\beta_1 = \beta_2 = 0.99$ and varying fractional orders $\alpha_1 = \alpha_2 = 0.99, 0.95, 0.90, 0.85$ the solutions are presented in Figures 3(c) and 3(d), highlighting the characteristics of fractional order calculus. Moreover, for a comprehensive comparison, solution plots of varying fractal and fractional orders along with the exact solutions, the solution plots are presented in Figures 3(e) and 3(f). A notable congruence has been noted between the exact solutions and solutions obtained via the $VLFF$ method, depicting the robustness and accuracy of the proposed numerical approach.

The error analysis is shown in Figure 7(a) which shows the validity of the $VLFF$ approach. These plots show the efficacy of the proposed $VLFF$ method in obtaining precise answers for $\psi_1(\xi)$ and $\psi_2(\xi)$. The solutions obtained by

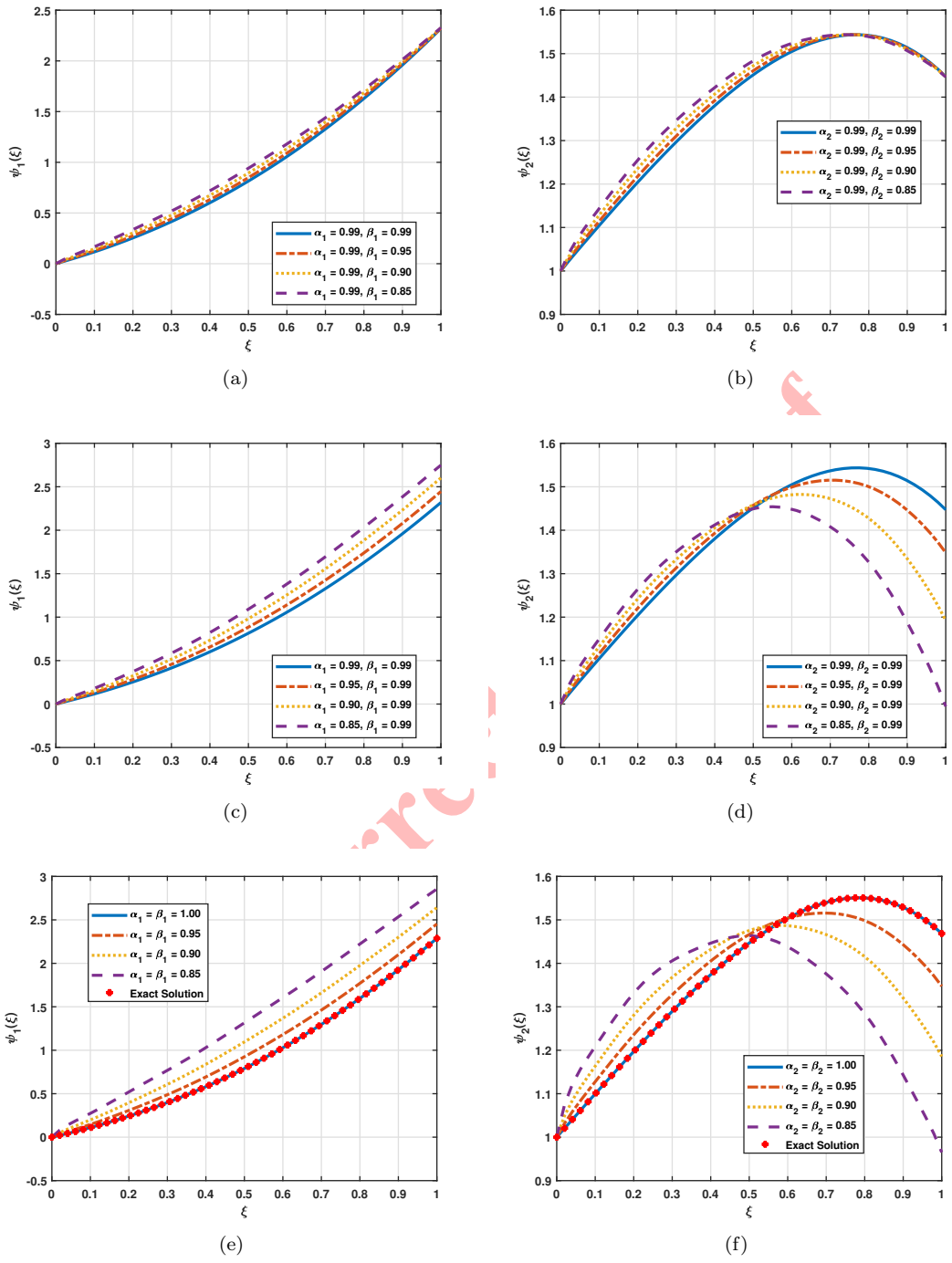

FIGURE 3. Solution plots for Example 5.1 at different values of α_1, α_2, β_1, and β_2.

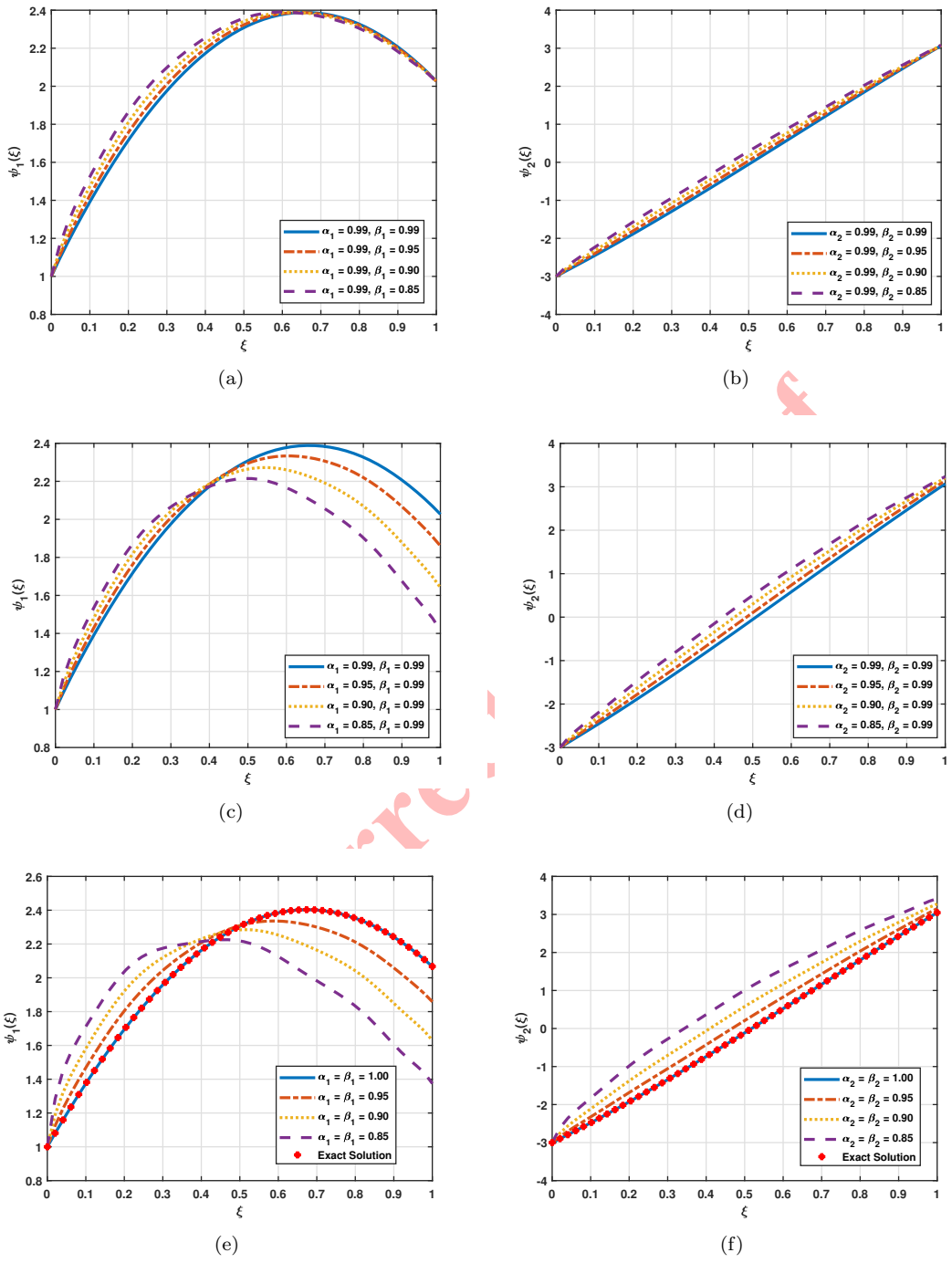

FIGURE 4. Solution plots for Example 5.2 at different values of α_1, α_2, β_1, and β_2.

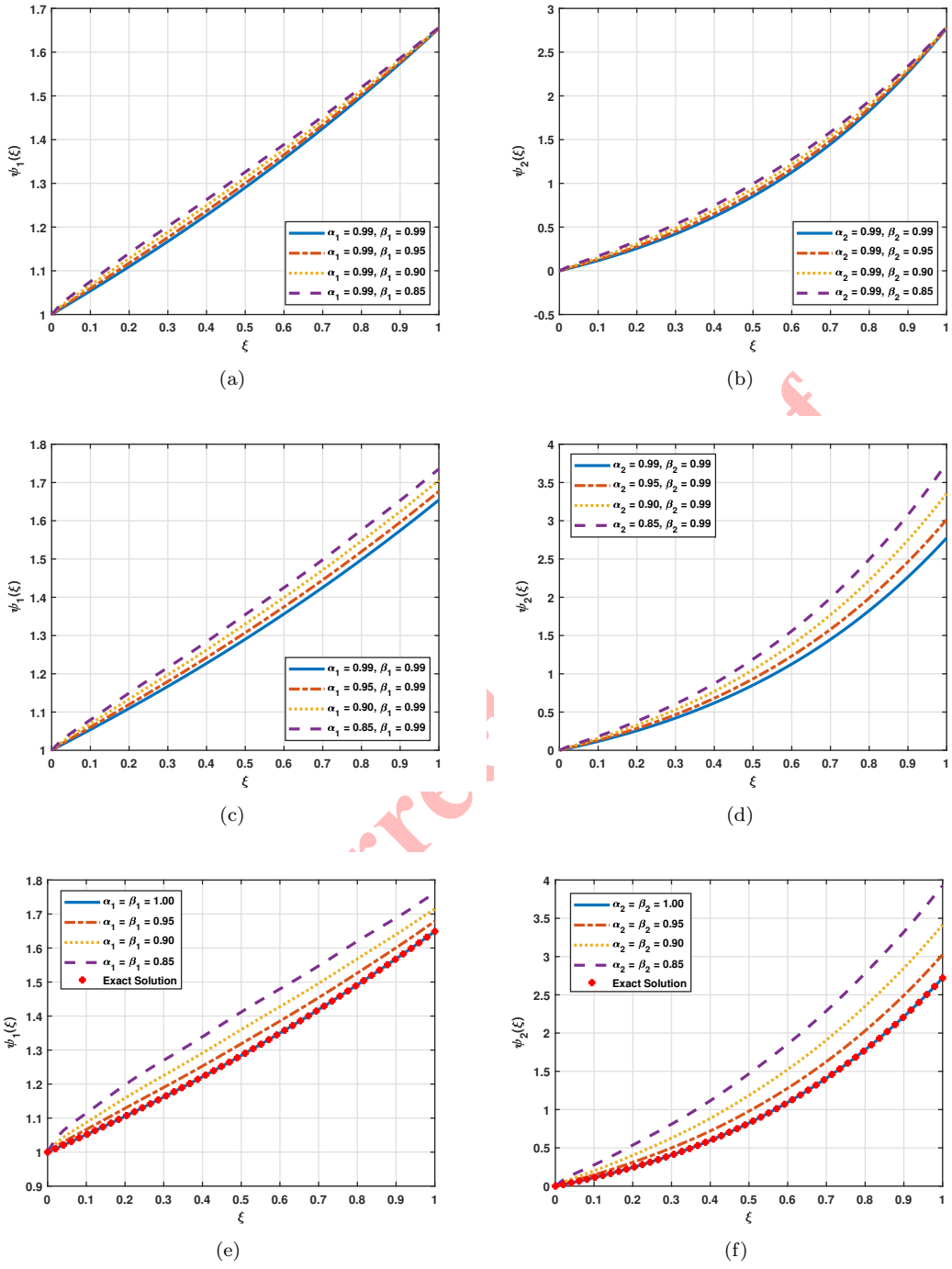

FIGURE 5. Solution plots for Example 5.3 at different values of α_1, α_2, β_1, and β_2.

TABLE 1. $VLFF$ solutions at different values of $\alpha_1, \alpha_2, \beta_1 \& \beta_2$ for Examples 5.1, 5.2, and 5.3.

ξ	$\psi_1(\xi)$			$\psi_2(\xi)$		
	$\alpha_1 = 0.99$			$\alpha_2 = 0.99$		
	$\beta_1 = 0.90$	$\beta_1 = 0.95$	$\beta_1 = 0.99$	$\beta_2 = 0.90$	$\beta_2 = 0.95$	$\beta_2 = 0.99$
Example 5.1						
0.0	0.00000	0.00000	0.00000	1.00000	1.00000	1.00000
0.1	0.14716	0.12929	0.11671	1.12848	1.11468	1.10470
0.2	0.30436	0.27523	0.25416	1.23585	1.21780	1.20424
0.3	0.47883	0.44199	0.41492	1.32828	1.31057	1.29698
0.4	0.67441	0.63254	0.60125	1.40713	1.39224	1.38044
0.5	0.89400	0.84901	0.81496	1.47225	1.46070	1.45133
0.6	1.13473	1.09055	1.05677	1.51728	1.51055	1.50492
0.7	1.39812	1.35849	1.32785	1.54058	1.53867	1.53681
0.8	1.68581	1.65385	1.62894	1.54050	1.54148	1.54201
0.9	1.99377	1.97446	1.95939	1.50949	1.51209	1.51406
1.0	2.32384	2.32100	2.31899	1.44660	1.44691	1.44710
Example 5.2						
0.0	1.00000	1.00000	1.00000	-3.00000	-3.00000	-3.00000
0.1	1.47290	1.42615	1.39174	-2.32124	-2.39811	-2.45302
0.2	1.81009	1.75696	1.71611	-1.68950	-1.80075	-1.88278
0.3	2.05459	2.01079	1.97614	-1.07245	-1.19709	-1.29049
0.4	2.22713	2.19774	2.17334	-0.45722	-0.58291	-0.67885
0.5	2.34153	2.32357	2.30808	0.16416	0.04198	-0.05227
0.6	2.38719	2.38243	2.37763	0.77113	0.66378	0.58042
0.7	2.37413	2.37978	2.38333	1.36765	1.28188	1.21461
0.8	2.31307	2.32106	2.32688	1.95954	1.89579	1.84559
0.9	2.19147	2.20009	2.20678	2.52526	2.49105	2.46426
1.0	2.02548	2.02640	2.02702	3.07652	3.07119	3.06738
Example 5.3						
0.0	1.00000	1.00000	1.00000	0.00000	0.00000	0.00000
0.1	1.06683	1.05934	1.05399	0.14759	0.12958	0.11693
0.2	1.12822	1.11741	1.10945	0.30737	0.27755	0.25604
0.3	1.18839	1.17617	1.16704	0.48868	0.45001	0.42174
0.4	1.24940	1.23682	1.22726	0.69779	0.65245	0.61878
0.5	1.31271	1.30010	1.29043	0.94060	0.89014	0.85220
0.6	1.37688	1.36535	1.35646	1.21777	1.16608	1.12681
0.7	1.44289	1.43320	1.42565	1.53505	1.48636	1.44895
0.8	1.51186	1.50428	1.49834	1.89904	1.85778	1.82578
0.9	1.58214	1.57779	1.57439	2.31153	2.28506	2.26447
1.0	1.65541	1.65474	1.65427	2.78106	2.77710	2.77432

the proposed $VLFF$ method are tabulated in Table 1, which depicts the solution values for $\psi_1(\xi)$ at $\alpha_1 = 0.99$ and $\beta_1 = 0.90, 0.95, 0.99$, and for $\psi_2(\xi)$ at $\alpha_2 = 0.99$ and $\beta_2 = 0.90, 0.95, 0.99$.

TABLE 2. $VLFF$ solutions at different values of $\alpha_1, \alpha_2, \alpha_3, \beta_1, \beta_2 \& \beta_3$ for Example 5.4.

ξ	$\psi_1(\xi)$		$\psi_2(\xi)$		$\psi_3(\xi)$	
	$\alpha_1 = 0.99$		$\alpha_2 = 0.99$		$\alpha_3 = 0.99$	
	$\beta_1 = 0.95$	$\beta_1 = 0.99$	$\beta_2 = 0.95$	$\beta_2 = 0.99$	$\beta_3 = 0.95$	$\beta_3 = 0.99$
0.0	1.00000	1.00000	1.00000	1.00000	0.00000	0.00000
0.1	1.12227	1.11092	1.25975	1.23430	0.41430	0.37153
0.2	1.24872	1.23099	1.55971	1.51581	0.94869	0.86704
0.3	1.38372	1.36230	1.91608	1.85711	1.65494	1.53316
0.4	1.53040	1.50676	2.34502	2.27283	2.59677	2.43150
0.5	1.69117	1.66614	2.86389	2.77998	3.85545	3.64387
0.6	1.86570	1.84145	3.48745	3.39735	5.52863	5.27723
0.7	2.05638	2.03468	4.23905	4.14970	7.75414	7.47828
0.8	2.26574	2.24801	5.14668	5.06706	10.7140	10.4443
0.9	2.49363	2.48289	6.23785	6.18408	14.6389	14.4373
1.0	2.74357	2.74211	7.55291	7.54530	19.8432	19.8130

Example 5.2. Take the system of FFDEs as follows:

$$\begin{aligned} {}_0^{Cff}D_\xi^{\alpha_1,\beta_1}\psi_1(\xi) + \psi_2(\xi) &= 1, \\ {}_0^{Cff}D_\xi^{\alpha_2,\beta_2}\psi_2(\xi) - \psi_1(\xi) &= 4, \end{aligned} \tag{5.3}$$

subject to

$$\psi_1(0) = 1, \psi_2(0) = -3. \tag{5.4}$$

The exact solution is given as $\psi_1(\xi) = 5\cos\xi + 4\sin\xi - 4$ and $\psi_2(\xi) = -4\cos\xi + 5\sin\xi + 1$.
The system of FFDEs shown in Example 5.2 has been solved using the proposed $VLFF$ method. Figure 4 shows the solution plots for $\psi_1(\xi)$ and $\psi_2(\xi)$ for several values of $\alpha_1, \alpha_2, \beta_1$, and β_2. For constant fractional orders $\alpha_1 = \alpha_2 = 0.99$ and variable fractal orders $\beta_1 = \beta_2 = 0.99, 0.95, 0.90, 0.85$, the solutions are illustrated in Figures 4(a) and 4(b). Similarly, for constant fractal orders $\beta_1 = \beta_2 = 0.99$ and variable fractional orders $\alpha_1 = \alpha_2 = 0.99, 0.95, 0.90, 0.85$, the solutions are illustrated in Figures 4(c) and 4(d). Figures 4(e) and 4(f) present the solution plots of different fractal and fractional orders with the exact solutions. The reliability and precision of the proposed numerical technique are shown by a notable alignment between the exact solutions and $VLFF$ solutions.
For Example 5.2, Figure 7(b) shows the error analysis therefore providing the efficacy of the $VLFF$ approach in resolving the solutions $\psi_1(\xi)$ and $\psi_2(\xi)$. These plots reveals the efficacy of the proposed $VLFF$ method in obtaining exact solutions for $\psi_1(\xi)$ and $\psi_2(\xi)$. The results derived from the suggested $VLFF$ approach are presented in Table 1, illustrating the solution values for $\psi_1(\xi)$ at $\alpha_1 = 0.99$ and $\beta_1 = 0.90, 0.95, 0.99$, as well as for $\psi_2(\xi)$ at $\alpha_2 = 0.99$ and $\beta_2 = 0.90, 0.95, 0.99$.

Example 5.3. Consider the system of FFDEs as:

$$\begin{aligned} {}_0^{Cff}D_\xi^{\alpha_1,\beta_1}\psi_1(\xi) &= \frac{\psi_1(\xi)}{2}, \\ {}_0^{Cff}D_\xi^{\alpha_2,\beta_2}\psi_2(\xi) &= \psi_1^2(\xi) + \psi_2(\xi) \end{aligned} \tag{5.5}$$

along with

$$\psi_1(0) = 1, \psi_2(0) = 0. \tag{5.6}$$

The exact solution is $\psi_1(\xi) = e^{\frac{\xi}{2}}$ and $\psi_2(\xi) = \xi e^{\xi}$.
The system of FFDEs shown in Example 5.3 has been solved using the $VLFF$ method. Figure 5 shows the solution

TABLE 3. A comparative analysis of error for Examples 5.1, 5.2, and 5.3.

	$\psi_1(\xi)$			$\psi_2(\xi)$		
ξ	Exact Solution	RK Error	$VLFF$ Error	Exact Solution	RK Error	$VLFF$ Error
Example 5.1						
0.0	0.00000	0	$1.48912e-16$	1.00000	0	$1.11022e-16$
0.1	0.11033	$3.43931e-09$	$2.93321e-13$	1.09965	$1.76606e-08$	$5.05429e-14$
0.2	0.24265	$2.12982e-08$	$1.06942e-13$	1.19706	$2.36473e-08$	$5.40457e-13$
0.3	0.39891	$1.08320e-07$	$2.96430e-13$	1.28957	$1.54081e-07$	$1.13864e-12$
0.4	0.58094	$2.59026e-07$	$3.24962e-13$	1.37406	$2.75611e-07$	$1.03406e-12$
0.5	0.79043	$4.72135e-07$	$4.37428e-14$	1.44689	$3.22800e-07$	$7.79377e-14$
0.6	1.02885	$6.88439e-07$	$2.83995e-13$	1.50386	$2.63760e-07$	$1.10800e-12$
0.7	1.29730	$1.42587e-06$	$3.30846e-13$	1.54020	$6.69151e-07$	$1.07603e-12$
0.8	1.59651	$1.72079e-06$	$1.66311e-13$	1.55055	$3.28418e-07$	$4.34763e-13$
0.9	1.92667	$1.97982e-06$	$9.14824e-14$	1.52891	$9.27048e-08$	$2.19380e-13$
1.0	2.28736	$2.23942e-06$	0	1.46869	$3.51110e-07$	$2.22045e-16$
Example 5.2						
0.0	1.00000	0	0	-3.00000	0	$4.44089e-16$
0.1	1.37435	$1.39672e-06$	$2.22045e-15$	-2.48085	$4.69781e-07$	$2.26485e-14$
0.2	1.69501	$3.17783e-07$	$3.55271e-15$	-1.92692	$5.10211e-07$	$4.28546e-14$
0.3	1.95876	$5.63101e-07$	$1.46549e-14$	-1.34374	$7.04517e-07$	$9.72555e-14$
0.4	2.16298	$1.15811e-06$	$1.86517e-14$	-0.73715	$8.15912e-07$	$9.31477e-14$
0.5	2.30561	$1.09642e-06$	$5.32907e-15$	-0.11320	$1.20882e-06$	$1.02696e-15$
0.6	2.38525	$5.51157e-07$	$1.33227e-14$	0.52187	$1.59830e-06$	$9.42579e-14$
0.7	2.40108	$1.53831e-07$	$1.86517e-14$	1.16172	$1.96014e-06$	$9.65894e-14$
0.8	2.35296	$7.49235e-08$	$1.11022e-14$	1.79995	$2.28264e-06$	$4.15223e-14$
0.9	2.24136	$3.13962e-07$	$7.10543e-15$	2.43019	$2.61637e-06$	$2.17604e-14$
1.0	2.06740	$6.68831e-07$	$8.88178e-16$	3.04615	$2.59899e-06$	0
Example 5.3						
0.0	1.00000	0	$1.33967e-08$	0.00000	0	$1.03756e-08$
0.1	1.05127	$1.83151e-08$	$1.02054e-08$	0.11051	$1.29377e-06$	$4.23081e-09$
0.2	1.10517	$6.34511e-09$	$1.00206e-08$	0.24428	$5.37760e-07$	$4.66222e-09$
0.3	1.16183	$7.09707e-09$	$1.07265e-08$	0.40495	$6.81697e-07$	$1.03957e-08$
0.4	1.22140	$7.58817e-09$	$4.59747e-09$	0.59673	$8.17180e-07$	$7.46643e-10$
0.5	1.28403	$1.29433e-08$	$1.36326e-08$	0.82436	$1.43979e-06$	$1.06893e-08$
0.6	1.34986	$2.05456e-08$	$5.07793e-09$	1.09327	$2.38265e-06$	$1.02593e-10$
0.7	1.41907	$2.79816e-08$	$1.06008e-08$	1.40963	$3.45137e-06$	$1.07489e-08$
0.8	1.49182	$3.58136e-08$	$1.04970e-08$	1.78043	$4.72009e-06$	$4.34854e-09$
0.9	1.56831	$2.90586e-08$	$1.03058e-08$	2.21364	$4.31732e-06$	$4.81617e-09$
1.0	1.64872	$2.61922e-08$	$1.38837e-08$	2.71828	$4.26196e-06$	$1.10395e-08$

plots for $\psi_1(\xi)$ and $\psi_2(\xi)$ for various values of $\alpha_1, \alpha_2, \beta_1$, and β_2. For fixed fractional orders $\alpha_1 = \alpha_2 = 0.99$ and variable fractal orders $\beta_1 = \beta_2 = 0.99, 0.95, 0.90, 0.85$, the solutions are depicted in Figures 5(a) and 5(b). Similarly, with fixed fractal orders $\beta_1 = \beta_2 = 0.99$ and varying fractional orders $\alpha_1 = \alpha_2 = 0.99, 0.95, 0.90, 0.85$, the solutions are depicted in Figures 5(c) and 5(d). Figures 5(e) and 5(f) present the solution plots of various fractal and fractional orders with the exact solutions. Notable congruence between the exact solutions and $VLFF$ solutions reveals the

TABLE 4. A comparative analysis of error for Example 5.4.

	$\psi_1(\xi)$		$\psi_2(\xi)$		$\psi_3(\xi)$	
ξ	*RK* Error	*VLFF* Error	*RK* Error	*VLFF* Error	*RK* Error	*VLFF* Error
0.0	0	$3.90230e-08$	0	$2.85421e-08$	0	$4.92228e-16$
0.1	$2.82408e-07$	$8.80651e-09$	$3.69314e-06$	$2.50222e-08$	$2.00927e-05$	$3.20277e-09$
0.2	$1.07368e-07$	$3.88332e-08$	$1.15302e-07$	$1.27413e-08$	$1.32661e-06$	$5.99662e-09$
0.3	$2.15358e-07$	$9.16095e-09$	$4.96353e-07$	$1.67644e-08$	$2.15881e-06$	$1.28201e-08$
0.4	$4.45915e-07$	$3.96394e-08$	$4.04212e-06$	$2.84452e-08$	$2.86100e-05$	$1.18092e-08$
0.5	$6.59226e-07$	$1.25571e-09$	$6.55052e-06$	$1.49414e-09$	$5.08185e-05$	$9.18136e-10$
0.6	$9.32919e-07$	$3.97393e-08$	$1.03808e-05$	$2.97236e-08$	$8.87297e-05$	$1.30222e-08$
0.7	$1.18545e-06$	$1.16447e-08$	$1.28156e-05$	$1.50792e-08$	$1.18031e-04$	$1.28074e-08$
0.8	$1.48077e-06$	$3.98920e-08$	$1.59271e-05$	$1.57000e-08$	$1.57934e-04$	$5.22085e-09$
0.9	$1.42764e-06$	$7.74430e-09$	$5.44856e-06$	$2.79820e-08$	$2.95607e-05$	$2.66455e-09$
1.0	$1.48648e-06$	$4.15379e-08$	$2.05760e-06$	$3.15387e-08$	$2.79060e-05$	0

reliability and accuracy of the proposed numerical method.
Figure 7(c) illustrates the error analysis, demonstrating the effectiveness of the $VLFF$ approach in ascertaining the solutions $\psi_1(\xi)$ and $\psi_2(\xi)$ for Example 5.3. The data demonstrate the efficacy of the suggested $VLFF$ technique in obtaining accurate solutions for $\psi_1(\xi)$ and $\psi_2(\xi)$. Table 1 showcase the results derived using the $VLFF$ approach illustrating the values for $\psi_1(\xi)$ at $\alpha_1 = 0.99$ and $\beta_1 = 0.90, 0.95, 0.99$, along with those for $\psi_2(\xi)$ at $\alpha_2 = 0.99$ and $\beta_2 = 0.90, 0.95, 0.99$.

Example 5.4. Here we take the system of FFDEs:

$$\begin{aligned} {}_0^{Cff}D_\xi^{\alpha_1,\beta_1}\psi_1(\xi) &= \psi_1(\xi), \\ {}_0^{Cff}D_\xi^{\alpha_2,\beta_2}\psi_2(\xi) &= 2(\psi_1(\xi))^2, \\ {}_0^{Cff}D_\xi^{\alpha_3,\beta_3}\psi_3(\xi) &= 3\psi_1(\xi)\psi_2(\xi) \end{aligned} \tag{5.7}$$

with

$$\psi_1(0) = 1,\ \psi_2(0) = 1,\ \psi_3(0) = 0. \tag{5.8}$$

The exact solution is $\psi_1(\xi) = e^{\xi}$, $\psi_2(\xi) = e^{2\xi}$ and $\psi_3(\xi) = e^{3\xi} - 1$.
The proposed $VLFF$ approach has been employed to address the system of FFDEs illustrated in Example 5.4. The solution curves for $\psi_1(\xi)$, $\psi_2(\xi)$, and $\psi_3(\xi)$ are presented in Figure 6 for different values of $\alpha_1, \alpha_2, \alpha_3, \beta_1, \beta_2$, and β_3. For constant fractional orders $\alpha_1 = \alpha_2 = \alpha_3 = 0.99$ and variable fractional orders $\beta_1 = \beta_2 = \beta_3 = 0.99, 0.95, 0.90, 0.85$, the solutions are illustrated in Figures 6(a), 6(b) and 6(c). Similarly with constant fractal orders $\beta_1 = \beta_2 = \beta_3 = 0.99$ and variable fractional orders $\alpha_1 = \alpha_2 = \alpha_3 = 0.99, 0.95, 0.90, 0.85$, the solutions are illustrated in Figures 6(d), 6(e) and 6(f), emphasizing the properties of fractional order calculus. Additionally, for an exhaustive comparison, solution charts of several fractal and fractional orders, together with the exact solutions, are illustrated in Figures 6(g), 6(h) and 6(i). A significant agreement has been seen between the exact solutions and those derived using the $VLFF$ method, illustrating the reliability and precision of the proposed numerical technique.
Figure 7(d) illustrates the error analysis, demonstrating the effectiveness of the $VLFF$ approach in ascertaining the solutions $\psi_1(\xi), \psi_2(\xi)$ and $\psi_3(\xi)$ for Example 5.4. The data demonstrate the efficacy of the suggested $VLFF$ technique in obtaining accurate solutions for $\psi_1(\xi), \psi_2(\xi)$ and $\psi_3(\xi)$. Table 2 presents the results derived from the proposed $VLFF$ methodology illustrating the solution values for $\psi_1(\xi)$ at $\alpha_1 = 0.99$ and $\beta_1 = 0.95, 0.99$, for $\psi_2(\xi)$ at $\alpha_2 = 0.99$ and $\beta_2 = 0.95, 0.99$, as well as those for $\psi_3(\xi)$ at $\alpha_3 = 0.99$ and $\beta_3 = 0.95, 0.99$. Additionally, Tables 3 and 4 illustrate the error produced by the $VLFF$ technique relative to the traditional fourth-order RK method. The $VLFF$ approach

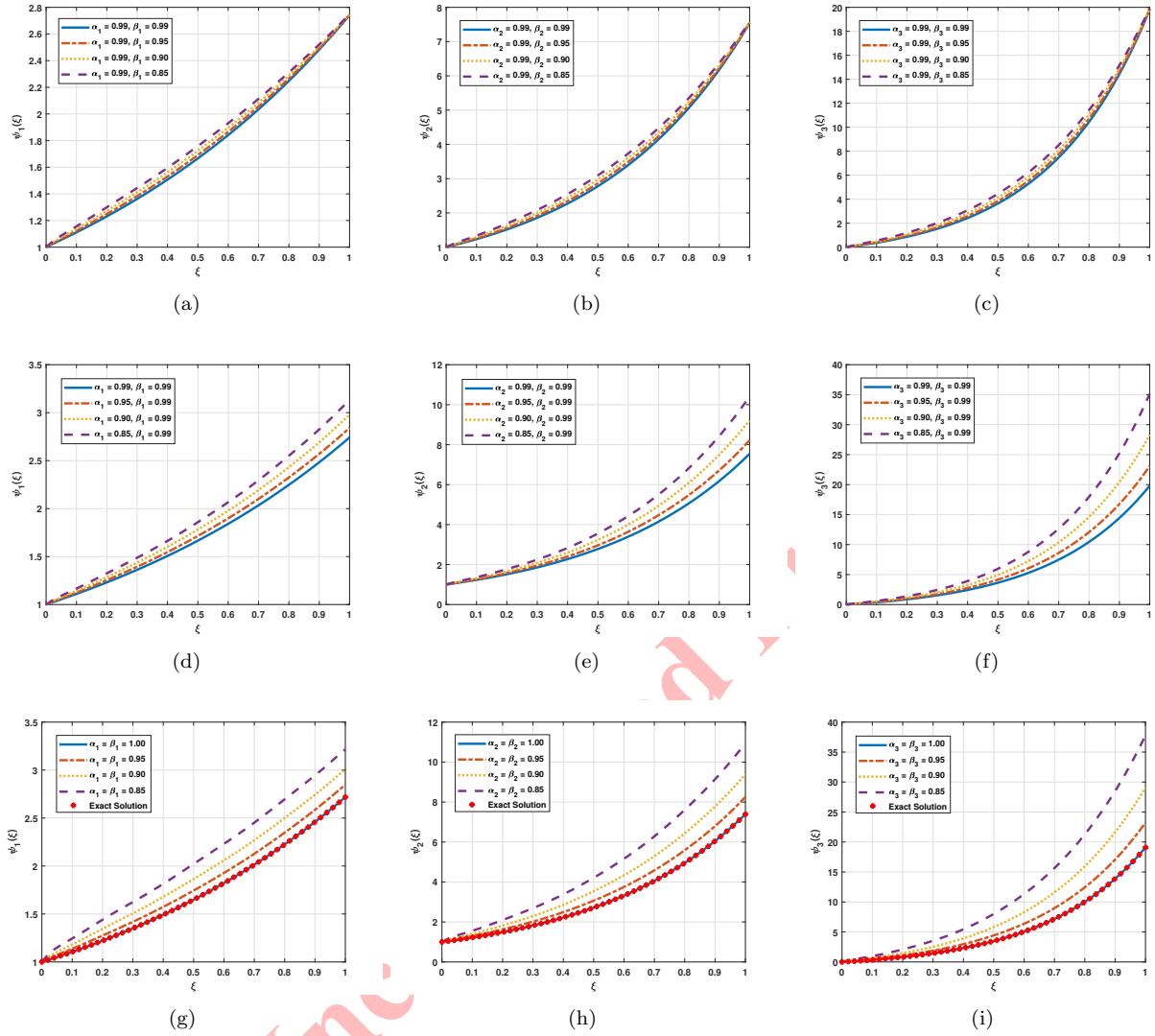

FIGURE 6. Solution plots for Example 5.4 at different values of α_1, α_2, α_3, β_1, β_2, and β_3.

demonstrated reduced error compared to the RK method. The numerical results show that the $VLFF$ method is a dependable, effective, and accurate method for solving the system of FFDEs.

6. Conclusion

The fractal-fractional differential equations find their applications in fields such as fluid dynamics, mathematical biology, physics, and engineering. In this study, a novel numerical scheme namely $VLFF$ method has been introduced to solve the system of fractal-fractional differential equations. The operational matrix of fractal-fractional orders was derived for the Vieta-Lucas polynomials and utilized further with the Tau method to handle the system of initial value FFDEs. Geometric representations of these fractal-fractional operational matrices were provided, depicting the fractal patterns. Empirical tests for validating the proposed $VLFF$ method incorporated figures and tables that demonstrate performance across various fractal and fractional orders. Results from the comparative study between the fourth-order

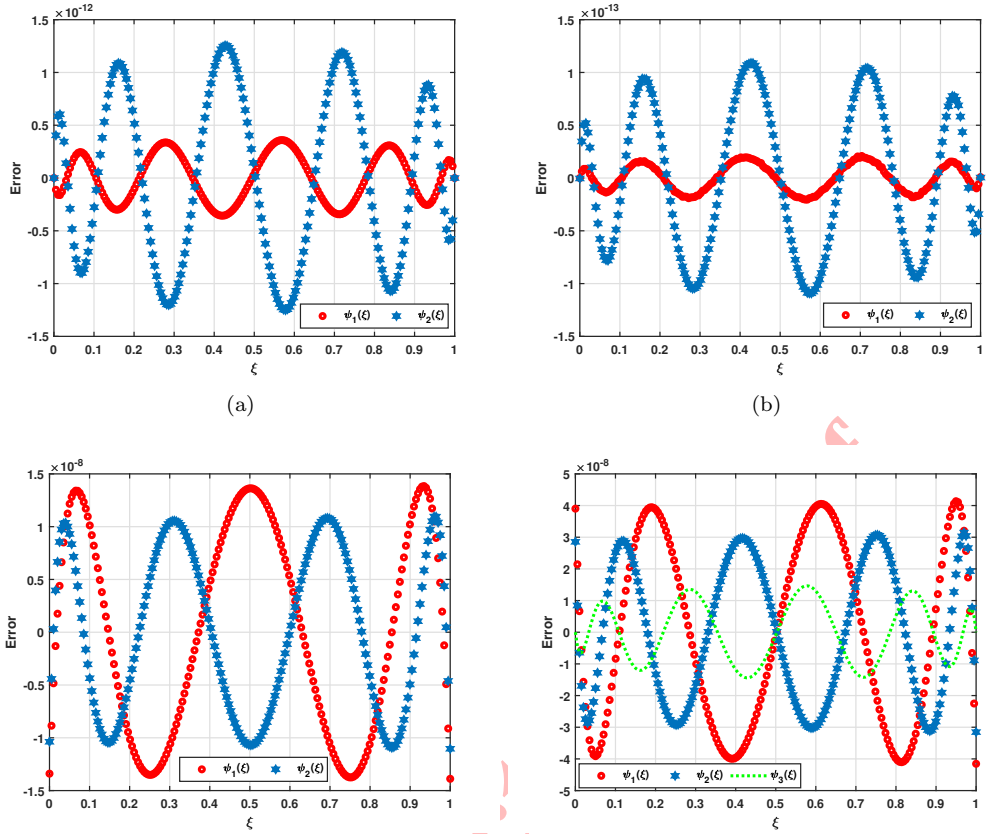

FIGURE 7. Error plots utilizing the $VLFF$ method for Examples 5.1, 5.2, 5.3, and 5.4.

Runge-Kutta method indicate that the $VLFF$ scheme offers superior precision and enhanced efficiency. Findings from this research study suggest that the $VLFF$ method has the potential to handle broader applications. In future, this method can be applied to examine complex systems comprising infectious disease models as well as real-world fractal-fractional dynamic systems.

ACKNOWLEDGMENT

The authors are deeply grateful to the editors for the positive response and also express thankfulness to the reviewers for carefully reading the paper towards the significant improvement in the quality and presentation of the manuscript.

REFERENCES

[1] T. Abdeljawad, M. Sher, K. Shah, M. Sarwar, I. Amacha, M. Alqudah, and A. Al-Jaser, *Analysis of a class of fractal hybrid fractional differential equation with application to a biological model*, Scientific Reports, *14*(1) (2024), 18937.

[2] P. Agarwal and A. A. El-Sayed, *Vieta–Lucas polynomials for solving a fractional-order mathematical physics model*, Advances in Difference Equations, *2020*(1) (2020), 1–18.

[3] S. Ahmad, K. Shah, T. Abdeljawad, and B. Abdalla, *On the approximation of fractal-fractional differential equations using numerical inverse Laplace transform methods*, CMES-Computer Modeling in Engineering & Sciences, *135*(3) (2023).

[4] A. Atangana, *Fractal-fractional differentiation and integration: connecting fractal calculus and fractional calculus to predict complex system*, Chaos, Solitons & Fractals, *102* (2017), 396–406.

[5] A. Atangana, A. Akgül, and K. M. Owolabi, *Analysis of fractal fractional differential equations*, Alexandria Engineering Journal, *59*(3) (2020), 1117–1134.

[6] R. Chaudhary, S. Aeri, A. Bala, R. Kumar, and D. Baleanu, *Solving system of fractional differential equations via Vieta–Lucas operational matrix method*, International Journal of Applied and Computational Mathematics, *10*(1) (2024), 14.

[7] M. H. Heydari, Z. Avazzadeh, and M. Razzaghi, *Vieta–Lucas polynomials for the coupled nonlinear variable-order fractional Ginzburg–Landau equations*, Applied Numerical Mathematics, *165* (2021), 442–458.

[8] M. H. Heydari, Z. Avazzadeh, and A. Atangana, *Shifted Vieta–Fibonacci polynomials for the fractal-fractional fifth-order KdV equation*, Mathematical Methods in the Applied Sciences, *44*(8) (2021), 6716–6730.

[9] A. F. Horadam, *Vieta polynomials*, Fibonacci Quarterly, *40*(3) (2002), 223–232.

[10] M. Jneid, M. Daher, M. Awad, and S. Marhaba, *A novel approach for time-local fractional solutions of certain nonlinear partial differential equations in fractal dimension*, International Journal of Analysis and Applications, *22* (2024), 207–207.

[11] M. A. Khan and A. Atangana, *Numerical methods for fractal-fractional differential equations and engineering: Simulations and modeling*, CRC Press, 2023.

[12] N. A. Khan, M. Ali, A. Ara, M. I. Khan, S. Abdullaeva, and M. Waqas, *Optimizing pantograph fractional differential equations: A Haar wavelet operational matrix method*, Partial Differential Equations in Applied Mathematics, (2024), 100774.

[13] R. Kumar, S. Aeri, and D. Baleanu, *Artificial neural networks for the wavelet analysis of Lane–Emden equations: exploration of astrophysical enigma*, International Journal of Modelling and Simulation, (2024), 1–12.

[14] S. Murtaza, P. Kumam, A. Kaewkhao, N. Khan, and Z. Ahmad, *Fractal fractional analysis of nonlinear electro-osmotic flow with cadmium telluride nanoparticles*, Scientific Reports, *12*(1) (2022), 20226.

[15] P. A. Naik, K. M. Owolabi, M. Yavuz, and J. Zu, *Chaotic dynamics of a fractional order HIV-1 model involving AIDS-related cancer cells*, Chaos, Solitons & Fractals, *140* (2020), 110272.

[16] P. A. Naik, M. Farman, A. Zehra, K. S. Nisar, and E. Hincal, *Analysis and modeling with fractal-fractional operator for an epidemic model with reference to COVID-19 modeling*, Partial Differential Equations in Applied Mathematics, *10* (2024), 100663.

[17] N. Pashmakian, A. Farajzadeh, N. Parandin, and N. Karamikabir, *A numerical approach for solving the fractal ordinary differential equations*, Computational Methods for Differential Equations, *12*(4) (2024), 780–790.

[18] S. Poojitha and A. Awasthi, *Operational matrix based numerical scheme for the solution of time fractional diffusion equations*, Fractional Calculus and Applied Analysis, *27*(2) (2024), 877–895.

[19] S. Shafipour and R. Katani, *Convergence analysis for piecewise Lagrange interpolation method of fractal fractional model of tumor-immune interaction with two different kernels*, Computational Methods for Differential Equations, *13*(1) (2024), 169–182.

[20] S. Sharma, A. Bala, S. Aeri, R. Kumar, and K. S. Nisar, *Vieta–Lucas matrix approach for the numeric estimation of hyperbolic partial differential equations*, Partial Differential Equations in Applied Mathematics, *11* (2024), 100770.

[21] S. M. Sivalingam, P. Kumar, V. Govindaraj, R. A. Qahiti, W. Hamali, and Z. M. Mutum, *An operational matrix approach with Vieta–Fibonacci polynomial for solving generalized Caputo fractal-fractional differential equations*, Ain Shams Engineering Journal, *15*(5) (2024), 102678.

[22] R. A. Silverman, *Special functions and their applications*, Courier Corporation, 1972.

[23] A. A. Taha and B. N. Abood, *Bernstein operational matrix for solving variable order fractional differential equations with generalized Caputo-type*, Wasit Journal for Pure Sciences, *3*(2) (2024).

[24] T. Taheri, A. A. Aghaei, and K. Parand, *Accelerating fractional PINNs using operational matrices of derivative*, arXiv preprint arXiv:2401.14081, (2024).